CrossMark

Future urban rainfall projections considering the impacts of climate change and urbanization with statistical–dynamical integrated approach

Hiteshri Shastri[1,2] · Subimal Ghosh[1,3] · Supantha Paul[1] · Hossein Shafizadeh-Moghadam[4] · Marco Helbich[5] · Subhankar Karmakar[1,6]

Abstract

Impacts of global warming and local scale urbanization on precipitation are evident from observations; hence both must be considered in future projections of urban precipitation. Dynamic regional models at a fine spatial resolution can capture the signature of urbanization on precipitation, however simulations for multiple decades are computationally expensive. In contrast, statistical regional models are computationally inexpensive but incapable of assessing the impacts of urbanization due to the stationary relationship between predictors and predictand. This paper aims to develop a unique modelling framework with a demonstration for Mumbai, India, where future urbanization is projected using a Markov Chain Cellular Automata approach, long term projections with climate change impacts are performed using statistical downscaling and urban impacts are simulated with a dynamic regional model for limited number of years covering different precipitation characteristics. The evaluation of the statistical downscaling methodology over historical time period reveals large underestimation of the extreme rainfall, which is improved effectively by applying another regression model, for extreme days. The limited runs of dynamic downscaling models with different stages of urbanization for Mumbai, India, reveal spatially non uniform changes in precipitation, occurring primarily at the higher quantiles. The statistical and dynamical outputs are further integrated using quantile transformation for precipitation projection in Mumbai during 2050s. The projections show dominant impacts of urbanization compared to those from large scale changing patterns. The uniqueness of this computationally efficient framework lies in an integration of global and local factors for precipitation projections through a conjugal statistical–dynamical approach.

1 Introduction

Characteristics of precipitation at global, sub-continental, regional and at a local scale has been affected, is being affected and will be affected by both global factors such as climate change (Milly et al. 2005; Zhang et al. 2007; Trenberth 2011) and local factors such as changes in Land Use

✉ Subimal Ghosh
subimal@civil.iitb.ac.in

1. Interdisciplinary Program in Climate Studies, Indian Institute of Technology Bombay, Powai, Mumbai 400 076, India

2. M. S. Patel Deartment of Civil Engineering, C. S. Patel Institute of Technology, Charotar University of Science and Technology, Changa, Anand, Gujarat, India

3. Department of Civil Engineering, Indian Institute of Technology Bombay, Powai, Mumbai, India

4. Department of GIS and Remote Sensing, Tarbiat Modares University, Tehran, Iran

5. Department of Human Geography and Spatial Planning, Utrecht University, Utrecht, The Netherlands

6. Centre for Environmental Science and Engineering, Indian Institute of Technology Bombay, Powai, Mumbai, India

Land Cover (LULC) (Schilling et al. 2010; Mahmood et al. 2010; Paul et al. 2016), urbanization (Huff and Changnon 1973; Kaufmann et al. 2007; Song et al. 2014), deforestation (Devaraju et al. 2015) etc. Global warming leads to increase in atmospheric moisture vapor at a rate of 7%/K; however models and observations indicate the increase in precipitation to be around 1–3% (Wentz et al. 2007). The change in precipitation is also not uniform around the globe. As for example the Indian Summer Monsoon Rainfall (ISMR) has a decreasing trend over last 50 years which is possibly associated with Western Indian Ocean warming and subsequent weakening of south westerly moisture flux (Roxy et al. 2015). Among the local factors, urbanization leads to the modification in urban micro climate in terms of generating Urban Heat Islands (Landsberg 1981) affecting the local convection by causing perturbation in wind circulation through changing resistance or generation of eddies (Oke 1987, 1995). This finally leads to intensification of extremes (Changnon et al. 1978; Huff 1986; Burian and Shepherd 2005). Global (Rosenfield 2000; Mishra et al. 2015) as well regional studies for the US (Jauregui and Romales 1996; Rose et al. 2008; Mishra et al. 2011), Europe (Trusilova et al. 2008; Kundzewicz 2010; Lasda et al. 2010) and India (Kishtawal et al. 2010; Vittal et al. 2013; Shastri et al. 2015) show this urban signature on intensified precipitation extremes. Hence, there is a need to consider the feedback from urban canopy in simulating urban precipitation.

Projections of climate variables, considering the increased Green House Gas emissions and associated radiative forcing, are performed with the General Circulation Models (GCMs). These climate change projections provide important information to the planners and policy makers for decision making under the rapidly changing climatic conditions (Mearns et al. 2012; Leung et al. 2003; Mujumdar and Ghosh 2008; Meehl et al. 2009). However, the resolution at which the GCMs operate (1°–2.5°, 100–250 km) is too coarse to resolve regional scale phenomenon such as clouds, topography and land surface processes that govern local climate (Hughes and Guttorp 1994; Giorgi and Mearns 1991; Ghosh and Mujumdar 2007; Salvi et al. 2013). The limitation of GCMs to provide meaningful climate projections at a regional scale has largely overcome by means of downscaling methods (Giorgi 2006; Hewitson and Crane 1996; Wilby and Wigley 2000; Salathé et al. 2007; Gutierrez et al. 2013). Downscaling refers to regional modeling of climate using the GCM outputs as boundary conditions.

Downscaling techniques are broadly classified into dynamic downscaling (DD) and statistical downscaling (SD). The DD models involve simulation of fine resolution atmospheric processes through Regional Climate Models (RCMs). The RCMs consider GCM simulations of synoptic scale circulations as initial and boundary conditions, incorporate the sub-grid scale features, and project climate

variables at a high resolution. The major drawback of DD is its complicated framework with multiple coupling between differential equations and high computational requirements, which restrict its use in long term climate change studies. The DD methodology remains inflexible in moving to a slightly different region as that requires redoing the entire experiment. Moreover, the large intermodal disagreement across different GCMs suggests the need of redoing of RCM simulations with different GCM input (Kharin and Zwiers 2002; Ghosh and Mujumdar 2007; Bellucci et al. 2015; Hwang and Graham 2014), which needs huge computational resources. On the other hand, SD establishes statistical relationship between large scale climate variables (or predictors) to regional or local scale variables (or predictands). They are computationally inexpensive. This makes SD widely acceptable for the multiple ensembles of GCMs for longer time periods and number of emission scenarios. The GCM output of long term climate change scenarios is used in the established statistical model to project the corresponding regional climate variables. The major limitation of SD methodology is the stationarity assumption. The methodology assumes that the relationship between the predictors and predictands will remain stationary, even in a changed climate (Wilby and Wigley 1997).

As the SD models are not based on physics, it is not possible to consider the feedback from the changing pattern of urbanization. The urban impacts can be considered in a DD framework (Lei et al. 2008). However, this needs very fine resolution simulations (preferably less than 5 km) over the urban regions to capture the urban feedback. Performing longer climate simulations at a multi-decadal (30 years) or century scale with future urbanization scenarios is impracticable, especially at a fine resolution and with multiple GCMs. Hence, the urban precipitation projections in the literature (Willems et al. 2012; Zahmatkesh et al. 2014; Chandra et al. 2015; Ahmadalipour et al. 2016) do not include the urban feedback. The projections, therefore, remain incomplete without considering the impacts of growing urbanization. This is more important in the developing countries such as India, where urbanization is taking place at a very fast rate (World Urbanization prospects 2014; Shafizadeh Moghadam and Helbich 2015). In India the impacts of urbanization is also visible in the changing patterns of rainfall extremes (Khishtawal et al. 2010; Vittal et al. 2013; Shastri et al. 2015).

To circumvent the identified limitations, this paper aims to develop a computationally efficient regional modeling framework for projection of urban precipitation considering the impacts of both global climate change and local urbanization growth. The proposed model has four modules. The first module deals with the assessment and projection of urbanization (urban LULC), where Markov Chain-Cellular Automata (MC-CA) approach has been used. The second

module uses SD methodology which has two sub-modules. The first sub-module uses conventional SD for regional projection of precipitation. The second sub-module is specifically for extreme days as the conventional SD models fail to simulate the extremes, though they are good for the mean precipitation conditions. The third module includes regional DD with Weather Research and Forecasting (WRF) model for limited number of years covering different characteristics of precipitation of the case study region. WRF is coupled with a very fine resolution (4 km) urban canopy model for considering the feedback from three urban LULC scenarios: observed conditions during 1972 and 2001 and projected condition during 2050. These DD simulations are essentially performed to understand impacts of urbanization. The fourth module integrates the outputs from module 2 and module 3. The changes in precipitation due to changes in LULC are obtained for different quantiles and applied to the SD model output. This is essentially quantile based change factor method and the final projection from the SD-dynamic model considers the impacts of both climate change and growing urbanization. We use the new generation Coupled Model Intercomparison Project 5 (CMIP5; Taylor et al. 2012) GCMs for the boundary conditions in implementing the proposed model. The city is prone to extreme monsoon rainfall due to its location at the wind ward region of Western Ghats hills of West coast of India.

2 Study region

The model is applied to the megacity Mumbai, India characterized through its rapid urban growth and extreme monsoon rainfall (UN urbanization prospect 2014). Mumbai is positioned at latitude 18.97°N and longitude 72.82°E on the western coast of India. The city comprises coastal lowland extending from the Arabian Sea in the west to the Western Ghats Escarpment (a mountain range covering 1,60,000 km^2 of area on the western coast of India) in the east. Mumbai is the financial and commercial capital of India popularly known as the powerhouse of the country. The city has experienced unexpected urban growth with the urban residents doubled from 8 to 16 million over the time period of 1971–2011 (Census of India 2011). At present, with around 21 million inhabitants, Mumbai ranks as 5th most populous urban region in the world, and the largest metropolitan region in India. The Mumbai Metropolitan Region (MMR) extends over an area of 4355 km^2 including its administrative limits covering Mumbai city (Greater Mumbai) and suburban districts. Figure 1a provides the location and extent of the Mumbai city and its suburban region under MMR. Nearly 45% area of MMR is below Mean Sea Level (MSL) comprising of Wetlands, including mangroves, tidal flats and salt pans.

Mumbai largely benefits from precipitation synoptically driven by high south-westerly flux and orographic factors. The station Santacruz-Mumbai measures an annual mean precipitation around 2100 mm. The precipitation over the city occurs during the monsoon season, June–September. The low lying geographical position and favorable rainfall conditions makes Mumbai flood prone. For example, between 2004 and 2007, during each monsoon, the city experienced heavy downpour events and related flooding (Gupta 2007). The city received incessant 944 mm of rain on 26 July 2005, causing loss of life of over 1000 people due to flood and associated catastrophes (Mathur and Sharma 2005). The significant heavy rainfall events in summer monsoon over Mumbai involve orographic uplift of the air masses coming from the Arabian sea, when they strike coastal ranges of Western Ghats. At the same time the observational and modeling studies suggests intensification

Fig. 1 Location of Mumbai and spatial extent of selected predictors. **a** Location of the city of Mumbai on the Western coast of India. The areal extent of Mumbai city and Mumbai Metropolitan Region (MMR) shown. **b** The extent of predictor region of the reanalysis and GCM data along with the location of Mumbai
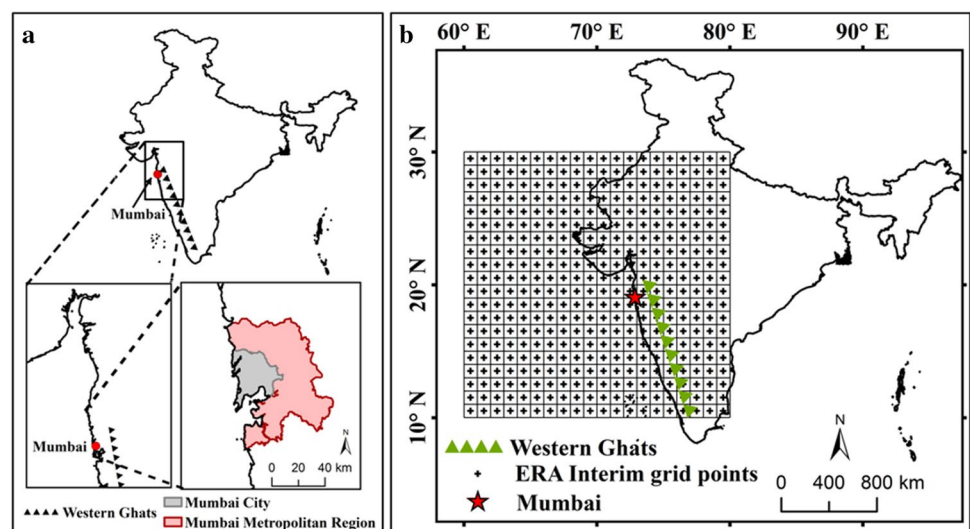
of heavy precipitation events over the city duo to growing urbanization (Shastri et al. 2015). Our objective here is to obtain the long term climate projections of occurrence of extreme rainfall return levels over the urban centre. Here we consider the global as well as regional drivers of extremes in terms of urban expansion of the city.

3 Method and data

The proposed methodology, for obtaining the urban rainfall projections considering impacts of climate change and urbanization, consists of four modules: (1) simulations of the urban growth in Mumbai, (2) SD model for climate change projections, (3) DD model for assessing impacts of urbanization, (4) integration of dynamic and statistical models. Figure 2 presents a schematic diagram of an overview of the integrated downscaling methodology. The following subsections discuss the different modules of downscaling methodology in details.

3.1 Module 1: simulating growth in urbanization

The first module of the proposed model addresses the growth of urbanization using the LULC maps derived from the satellite data (1973–2010) and a Markov Chain Cellular

Automata (MC-CA) model to obtain future LULC during 2050. MC-CA is a popular approach used for urban growth modelling (Kamusko et al. 2009; Guan et al. 2011; He et al. 2013; Eastman 2009). Supplementary Figure S1 presents an overview of different steps involved in the simulation of urban growth. We collect the satellite information pertaining to the urban growth of the city of Mumbai from 1973 to 2010 and use a predictive model to obtain future LULC during 2050 using integrated Markov Chain Cellular Automata (MC-CA) model. The MC-CA model projects the future urbanization based on the retrospective LULC data (Shafizadeh Moghadam and Helbich 2013). The methodology involves (a) satellite image classification, (b) determination of transition probability maps based on the driving forces of urban growth, using Multi Criteria Evaluation (MCE), and (c) projection of the urban growth using the CA model.

The Landsat satellite imageries available through the Global Land Cover Facility repository (http://www.landcover.org) are obtained over the years: 1973, 1990, 2001 and 2010 for spatiotemporal LULC mapping. At the first step of satellite image classification, geometrical corrections (rectification or resampling) are carried out. The geometric correction is applied to match the location of each pixel in such a way that it fits to the projection of reference map or image. This is particularly important when the comparison of individual pixels between two or more satellite images, such as change
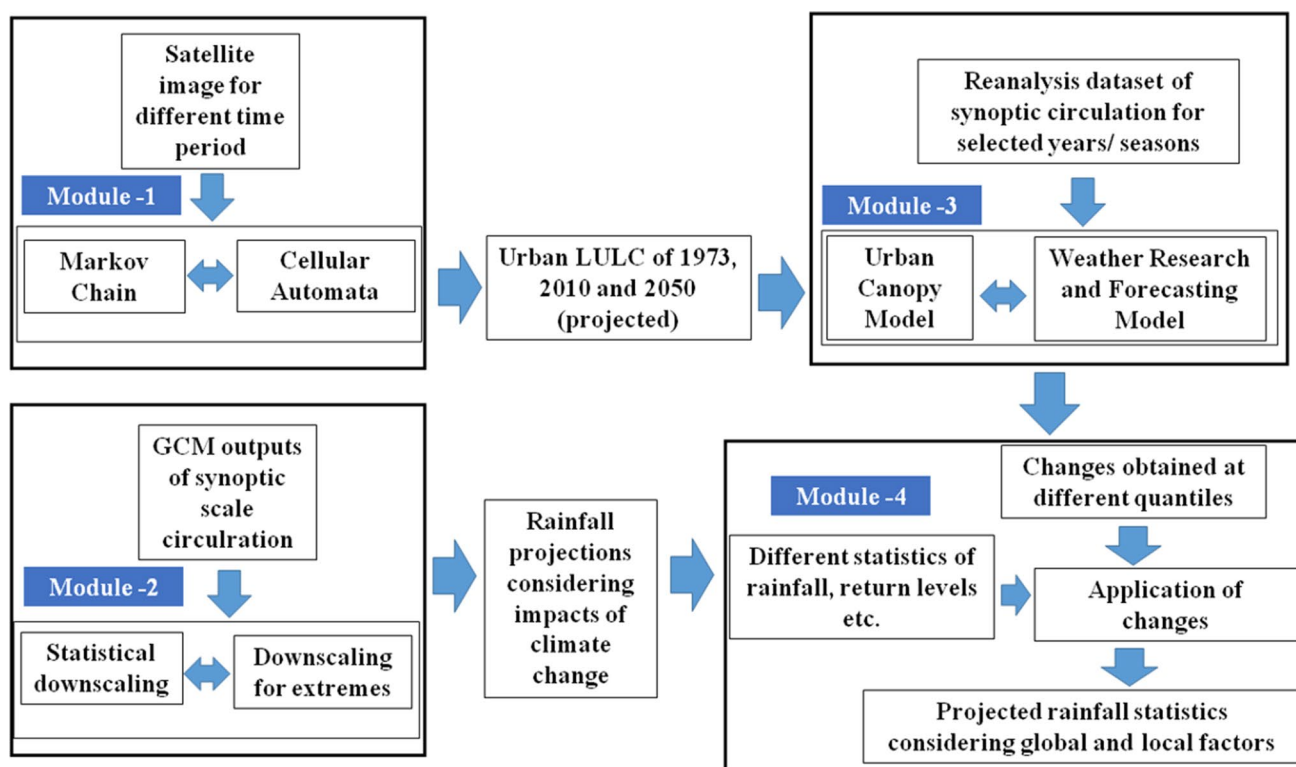

Fig. 2 A schematic diagram for an over view of the developed methodology

detection is aimed. The classified LULC maps are obtained based on the maximum likelihood algorithm (Schowengerdt 2012). The LULC maps discriminates five land use categories namely, built up areas, open land and cropland, forest and green space, wetlands, and water bodies. The classification is manually improved in a post-processing step. The classification is evaluated with a visual verification of a random well distributed sample of size 250 with Google Earth, open street map and official reference maps. The statistical evaluation of the classification accuracy is carried out using the kappa coefficient (Cohen 1968). The kappa coefficient is defined as the ratio between the numbers of correctly classified samples (the diagonal elements in the error matrix) and the total number of samples (Kraemer 1982; Pontius et al. 2004).

The factors affecting land use transition probabilities are identified based on previously performed studies (He et al. 2013; Azari et al. 2016). The study utilizes three auxiliary datasets namely population information (United Nations 2011; Census of India 2001,2011) transportation network map [obtained from the Open Street Map (OSM)] and ASTER digital elevation model (Tachikawa et al. 2011).

GIS algorithms are applied to derive slope from the ASTER digital elevation model and to obtain Euclidean distances to wetlands, water bodies, roads, and built-up areas, and subsequently they are used for computing transition probability maps with MCE (Shafeezadeh Moghaddam et al. 2017). The selected auxiliary variables are used in an analytical hierarchy process (AHP) (Saaty 1990) framework with a relative importance (weight) to each criterion. AHP assigns weights to the driving forces of urban growth. The weights of different auxiliary variables are determined based on expert knowledge and the published literature (Araya and Cabral 2010). The auxiliary variables with higher weights are more important. The consistency ratio is calculated to verify the consistency of the assigned weights. MC model is further linked to the AHP. Based on the past data, MC quantifies the rate of changes in the future. The values predicted by the MC and AHP are finally used as input to the CA model (White and Engelen 1997). Here, the CA performs the spatial allocation and location of change. Model validation is performed to ensure that it effectively predicts the future urbanization. The model is validated by comparing the simulated urban growth map of 2001–2010 with the observed one. The validated model is employed to obtain the simulations of future patterns of urban expansion for the year 2050. The simulated built-up areas for 2050 is tested using the point pattern analyses (Helbich 2012).

3.2 Module 2: statistical downscaling (SD) model for climate change projections

The second module deals with the assessment of global climate change impacts on regional urban precipitation. This particular module has two sub-modules. The first sub-module is a conventional SD model using linear regression for projection of daily rainfall. The second sub-module deals with extreme days for a better projection of extreme rainfall events.

3.2.1 Projection of daily rainfall

Here we follow the methodology used by Kannan and Ghosh (2013) and Salvi et al. (2013), but for single site. The methodology involves derivation of statistical relationship between the synoptic scale climate variables forming the synoptic scale circulation patterns and the observed rainfall over Mumbai city. The statistical relationship is then applied to the bias corrected GCM outputs for projections of urban precipitation. The stepwise methodology for projection of urban precipitation is presented in Supplementary Figure S2. The development of statistical relationship involves multiple steps, viz., standardization, principal component analysis and linear regression. First we present a brief description of variables used.

The rainfall data are collected from Indian Meteorological Department (IMD) for the station at Santacruz located in the Mumbai. For this study we use continuous records of 39-years (1969–2007) for 24 h accumulated precipitation measurements at 08:30 LT. The precipitation data pertaining to the Indian Summer Monsoon months (122 days of June–September, JJAS) are delineated from the annual data. The days with missing rainfall records are omitted from the 39-year JJAS continuous rainfall time series, when we develop the statistical relationship.

The selection of coarse resolution predictor data is an important step in SD models as they form the synoptic scale circulation pattern and plays important role in the performance of the SD model. Predictors should be so chosen such that they are related to precipitation, they are reliably simulated by GCMs and carry the signal of climate change in their changing patterns. Humidity plays an important role in capturing changes in water holding capacity of atmosphere under global warming (Wilby and Wigley 1997). Temperature, U wind, V wind and pressure add considerable power to predict short and long term variabilities and changes in precipitation. The predictors selected for this analysis are air temperature, wind velocities (U and V wind), mean sea level pressure, and specific humidity; at 1000 hPa level. In addition to them, the 500 and 850 hPa level U and V wind velocities are included as predictors, because these higher level variables are associated with monsoon circulation and hence important for simulating precipitation in Mumbai.

The selected predictors are obtained from ERA-interim, provided by European Centre for Medium-range Weather Forecasts (ECMWF) (Dee et al. 2011), reanalysis data set at daily scale. The reanalysis data at a resolution of 1°

latitude × 1° longitude grid is obtained for a region, extending from latitude 10° to 30°N and longitude 60° to 80° E. This spatial domain of the predictors is selected over large part of the Indian sub continental land and Arabian Sea to consider land–ocean thermal gradient and south westerly moisture flux from ocean towards monsoon rainfall around the city of Mumbai. The key source of rainfall in coastal city of Mumbai is the moisture flux from Arabian Sea. Hence, we select the predictor region slightly more extended towards the Arabian Sea. Figure 1b provides the location of Mumbai city on the map of India along with spatial extent of ERA Interim reanalysis grid points (21 × 21; total 441 grid points). The base line period considered for the present study is from 1979 to 2007 which is of sufficient duration to establish a reliable climatology (Ghosh and Mujumdar 2007, Salvi et al. 2013).

The GCM (CMIP5) outputs for the same predictors are obtained from the database of the World Climate Research Programme, Program for Climate Model Diagnosis and Inter-comparison (PCMDI). The two GCMs selected for the current study are: Canadian Centre for Climate Modeling Analysis (CCCMA) and Centre National de Recherches Meteorologiques (CNRM-CM5). These models are reasonably good in simulating Indian Summer Monsoon Rainfall (ISMR) during historical period of post 1950 (Saha et al. 2014). Table 1 lists the model name, institution and horizontal resolution of atmospheric component. The impacts of climate change on the precipitation characteristics for the year 2030–2050 is examined under the two Green House Gas emission scenarios namely Representative Concentration Pathway (RCP)4.5 and RCP8.5 (Moss et al. 2010; Vuuren et al. 2011). The future period considered for this analysis is 2030–2050 (21 years) and the projected changes are computed with respect to the base line period 1985–2005 (21 years).

The GCM-projected/reanalysis data (predictors) and the observed rainfall (predictand) undergo different mathematical operations before being statistically linked with each other. The predictors simulated by GCMs undergo bias correction operation. The bias correction operation removes systematic error in GCM predictor variables with respect to the reanalysis data using a quantile-based remapping technique (Li et al. 2010). A detail description of bias correction methodology is presented in the supplementary information S3. Principal component analysis (PCA) is applied to the bias corrected predictors. PCA performs an orthogonal transformation on the set of correlated predictors, producing dimensionally reduced, uncorrelated principal components (PCs). The PCs with a lower dimension carry nearly the same variability as that of the high dimensional original data. The daily observed rainfall data and obtained PCs of the predictor variables are the inputs to the regression model. The statistical downscaling model uses 265 PCs having 98% explained variance. PCs from reanalysis data and observed rainfall, for the training period, are used for deriving the statistical relationship. Performance of trained model is evaluated over the testing time period. We apply the tested liner regression model to the PCs obtained from GCM simulated predictors for the projection of rainfall. The time window 1979–1993 (15 years) is considered as the training period and the period, 1994–2007 (14 years) is considered as the testing period for the regression model. Here, it is important to mention that the length of model training time period is limited with the availability of data. With a higher length of training data set, development of more robust model is possible. However, length of training data set considered with this study (14 years) is sufficient duration to establish a reliable climatology (Ghosh and Mujumdar 2007; Salvi et al. 2013; Kannan and Ghosh 2013). The tested model is then applied to the historic GCM datafor the time period 1985–2005. The historical time period is selected as 1985–2005. This is considered as the reference period with respect to which the future changes are computed. As this period also belongs to historical period of CMIP5 platform, it is termed as "historic".

Validation of a downscaling model is an essential step to ascertain the performance of downscaling procedures. Here, the validation of proposed SD model is carried out by comparing the statistical properties of observed rainfall data of station Santacruz (Mumbai) and simulated historical rainfall time series (1985–2005) with GCM outputs (historical data) as predictors. Future projections of rainfall are generated; with the help of pre-established relationships applied to the predictors for the same period. The future projections are obtained for time period 2030–2050 for RCP4.5 and RCP8.5 scenarios.

Table 1 Description of GCMs used in the study

Sr. no.	Institution	Coupled model	AGCM resolution Lon. × Lat.	Ensemble no.
1	Canadian Centre for Climate Modelling and Analysis (CCCma)	CanESM2	2.8125° × 2.8125°	5
2	Centre National de Recherches Meteorologiques/Centre Europeen de Recherche et Formation Avancees en Calcul Scientifique (CNRM-CERFACS)	CNRM-CM5	1.40625° × 1.40625°	1

3.2.2 Projection of extreme rainfall

Conventional regression based downscaling methods are good for projecting mean conditions, but they cannot simulate extreme rainfall events with the same skill (Wilby et al. 2004; Benestad and Mezghani 2015; Kannan and Ghosh 2013). Hence, the extreme events need special treatment in the downscaling framework. Here, for extreme events, we extract the days with extreme rainfall (above 95th percentile) and apply a separate kernel regression model only for those days. We first obtain the rainfall time series from standard statistical downscaling and obtain the extreme days considering 95th percentile as threshold. We then use another regression specifically for those extreme days. This procedure is applied to training dataset (period: 1979–1993) and the regression coefficients/parameters thus obtained are applied to the testing (period: 1994–2007) with vector the selection of extremes in an intermediate step. The detailed methodology for extreme statistical downscaling is available in Shashikanth and Prashanthi (2018). Testing, validations and projections of the extreme rainfall with kernel regression model are performed. The reason behind the use of kernel regression is to capture a possible non-linear relationship between predictor and predictand, which may exist due to complex processes associated with extreme rainfall during monsoon.

3.3 Module 3: dynamic downscaling (DD) model for assessing impacts of urbanization

We perform the dynamic downscaling (DD) to understand the impact of urbanization on rainfall over Mumbai. The state-of-the-art numerical atmospheric model WRF is employed for this study. WRF model is widely used for idealized atmospheric simulations as well as operational forecasts. The WRF is a non-hydrostatic, compressible atmospheric model capable of forecasting using real-time data or idealized atmospheric simulations (Skamarock and Klemp 2008; Skamarock et al. 2012). Here, three different experiments are conducted with WRF coupled with Urban Canopy Model (UCM) (Chen et al. 2011; Kusaka et al. 2012) over the city of Mumbai. The three WRF–UCM experiments, performed here, consider observed urban expansion of the city during 1973, 2001 and the projected urban LULC during 2050. The LULC maps for 1973, 2001 and 2050 are obtained from module 1. Supplementary Figure S4 enlists different steps involved with the DD methodology.

We use the ERA-Interim reanalysis data (Dee et al. 2011) from the European Centre for Medium-range Weather Forecasts (ECMWF) for regional simulation of rainfall. The ERA-interim is a post satellite period data with a better quality (Kannan et al. 2014). We use 6-h reanalysis data (00, 06, 12, 18 UTC) at a spatial resolution of 0.75°×0.75° over

30 pressure levels for this experiment. The coarse domain consists of 74×93 grids, whereas the inner most domain has a 232×304 mesh covering the Mumbai and its surroundings with a spatial resolution of 4 km. The coarse domains derive the LULC information from MODIS land cover map. We prepare three different land cover maps to represent pre urbanization (LULC 1973), current urbanization (LULC 2001) and future urbanization (LULC 2050) over the city of Mumbai as obtained from module 1.

WRF model version 3.6 is used for the regional simulations. The basic steps of numerical modelling with WRF involves the input data pre-processing, numerical model simulations, validation of the post-processed model output and analysis of the outputs using statistical methods. The pre-processing involves converting the input reanalysis data into a WRF readable format. The WRF pre-processing system (WPS) prepares the domains with static and meteorological data for the model run through the method of nesting. We perform the simulations over the Mumbai metropolitan area using three nested domains. The WPS domain configuration is shown in Fig. 3. The resolutions of three domains d01, d02, d03 are 36 km, 12 km, and 4 km, respectively. During the model run, the downscaling occurs first in the coarsest nest followed by finer nests. In order to get optimal results from WRF model, it has to be configured with the best suitable parameterization schemes and physics suitable in the particular climatology. Tailoring of these physics combinations is done by following the previous experimental studies conducted by Shastri et al. (2015) and Paul et al. (2016, 2018). Brief information of physical parameterizations used for the present WRF simulation is presented in Table 2.

In order to represent the physical processes involved in an urban environment, i.e., the exchange of heat, momentum, and water vapor, WRF is coupled with an Urban Canopy Model (UCM) (Kusaka et al. 2001). The UCM consider the urban feedback to the wind, temperature, humidity, and its influence on the urban boundary layer (Kusaka et al. 2001). The coupled model improves the description of lower boundary conditions and provides more accurate projection for urban regions (Holt and Pullen 2007; Miao et al. 2011; Lin et al. 2011; Ganeshan et al. 2013). The single layer UCM with a simplified urban geometry is employed in this study. The anthropogenic heat (AH) flux with DD is taken care by the coupled WRF–UCM model. The coupled modelling framework consists of a suite of urban parameterization that incorporates AH. AH flux differs with the input fine scale classified LULC data of three land-cover cases. The coupled WRF–UCM has been compiled on an IBM cluster to obtain the projections. The model output is extracted for visualization and spatial analysis of simulation results.

We perform the regional simulations with WRF for 10 years of monsoon season to understand the impacts of urban expansions on the precipitation process. For selecting
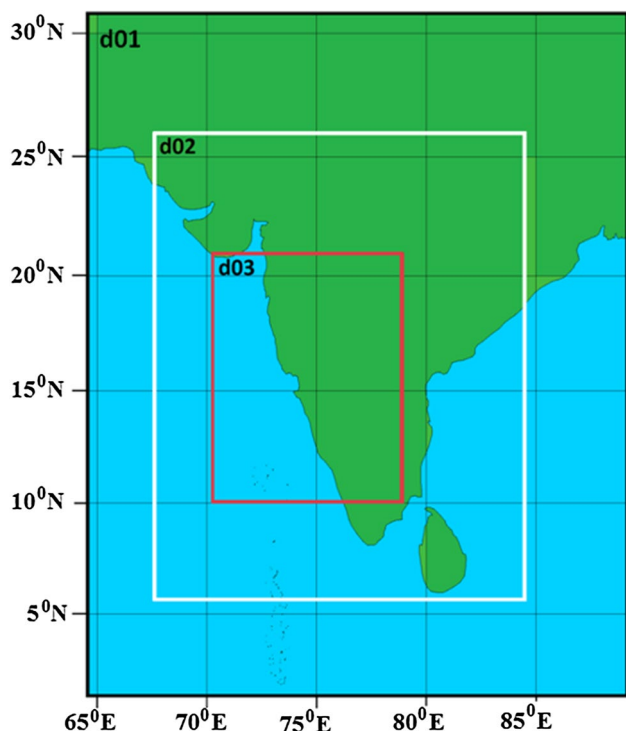
Fig. 3 Configuration of the WRF–UCM model simulation domains. Domains for WRF–UCM simulation: domain 1 (denoted d01, resolution 36 km), domain 2 (denoted d02, resolution 12 km) and domain 3 (denoted d03, resolution 4 km). Domain 3 is focused on urban feedback and is shown with red rectangle

the time period of dynamic simulation, we computed the standard deviation of observed rainfall data of Santacruz (Mumbai) with a 10 years moving window run over the period 1969–2007. We find that the period from 1997 to 2006 has the highest variability of rainfall and hence, it is selected for dynamic simulations. We perform the WRF simulation for three different urban development cases, namely pre urbanization (1973), current urbanization (2001) and projected urbanization (2050). Though the continuous simulations are better, they are avoided here because of huge

computing requirements. Literature suggests that 1 month spin up is sufficient for regional land–atmosphere simulations (Giorgi and Mearns 1999). 20 day spin-up time was used for the seasonal simulations of Indian monsoon rainfall performed by Srinivas et al. (2013). Here, we have used 1 month spin-up, similar to recent studies on monsoon simulations (Paul et al. 2016; Devanand et al. 2017). The differences obtained between the simulations provide the impacts of growth of urbanization on precipitation characteristics.

3.4 Module 4: integration of dynamic and statistical models

This module deals with the integration of both statistical and dynamic model. The output of SD model (Module 2) provides the basic statistics of the projected rainfall, e.g., mean and standard deviation. Regression for extreme days projects the extreme rainfall, which are further used in deriving the return levels corresponding to a specific return period, to understand the projected changes in design rainfall. We use the extreme value theory (EVT) for the same, which infers the tail behavior of a population, for example 100-year return levels (or, 1% probability storms). An overview of this module is given in Supplementary Figure S5.

The annual maxima (AM), and the peaks-over-threshold (POT) approaches are two popularly used methods based on EVT to obtain the return level of extreme hydrologic events. Here we use the POT approach to obtain the 50 years extreme rainfall return level for the city of Mumbai. Following POT approach, we retain all the peak values exceeding a certain threshold.

Normally, a Generalized Pareto Distribution (GPD) (Pickands 1975; Davison and Smith 1990) is fitted to these peaks. If GPD does not show a good fit with Kolmogorv–Srimonov (K–S) test, we apply nonparametric kernel density function. The return levels are obtained from the corresponding CDFs with the fitted distribution. Details may be found in Coles et al. (2001) and Vittal et al. (2013). Two important parameters used in the POT approach are the threshold 'u' and

Table 2 WRF model configuration and setup	Physics	Setup
	Cloud micro physics	Thompson scheme (Thompson et al. 2008)
	Sub grid scale cloud	Kain–Fritsch (new Eta) scheme (Kain 2004)
	Boundary-layer	Mellor–Yamada–Janjic TKE scheme (Janjic and Zavisa 1994; Janjic 1994, 2002)
	Long wave radiation	RRTM scheme (Mlawer et al. 1997)
	Short wave radiation	Dudhia scheme (Dudhia 1989)
	Surface-layer	Monin–Obukhov–Janjic scheme (Monin and Obukhov 1954, Janjic 1994)
	Land-surface	Unified Noah land-surface model (Tewari et al. 2004)
	Urban parameterization	Single-layer, UCM (Kusaka et al. 2001)

the minimum time span of extremes, ∆t. The assumption of the method is that extreme values are serially non-auto-correlated. Both, the truncation value and the time span of occurrence of extreme event, affect the results in terms of the frequency and the exceedance estimates (Coles et al. 2001). Here, we consider the threshold as the 95th percentile value of the rainfall time series for the present case-study. The value of ∆t is selected as 1 day; same as the physical time interval of the two consecutive observations. We use the standard Ljung–Box Q-test for the autocorrelation among residuals for the selected successive storm observations and make sure significant autocorrelation does not exist. This methodology is used to calculate the return levels for each of the selected GCMs and three scenarios (historical, RCP 4.5 and RCP 8.5).

We estimate the 50 years flood return levels with POT method using GPD with the statistically downscaled projections obtained with both GCMs and three scenarios. From module 3 we find the changes in precipitation characteristics due to projected growth of urbanization with the simulations from limited number of years. As these years are selected to cover highest variability of precipitation, it can be assumed that the changes computed in terms of differences in simulated precipitation for different urbanization represent the impacts of growth of urbanization. We compute the changes for different quantiles from the WRF–UCM simulations. We then apply the same changes to the projections obtained from module 2 at different quantiles. The procedure is very similar to the procedure which was used by Li et al. (2010) for climate change impacts assessment. The Supplementary information S3 presents a detail description of quantile based integration methodology. The time series after applying the changes represent the projections of precipitation considering both global and local factors. POT is further applied to these time series to compute the changed return levels of extreme. The statistical and dynamic downscaling methods are applied independently and hence, their calibration/validation periods are also independent.

The training and testing period for the statistical downscaling procedure is selected in a sequential manner. The length of training/testing time period is selected based on the availability of observed rainfall (39-years: 1969–2007) and the large scale climate circulation (ERA Interim) data (29-years: 1979–2007). With a higher length of training data set, development of more robust model is possible. The next section presents the results obtained with this methodology.

4 Results

The result section presents the outcome of the four methodology modules with the following subsections.

4.1 Module 1: simulating growth in urbanization

The image classification is performed for the satellite images of 1973, 1990, 2001 and 2010 and that resulted LULC maps of four different periods comprising built up areas, open land and cropland, forest and green space, wetlands, and water bodies. The statistical accuracy assessment of the manually improved classification is obtained through the kappa coefficient. The values of kappa coefficient for classified satellite images of all the four selected timestamps (1973, 1990, 2001 and 2010) are within the range of 0.84–0.86. The coefficient values indicate fair classification accuracy for further use of classified data. The extracted LULC maps for 1973–2001 are illustrated in Fig. 4a, b respectively. Here, we may clearly notice a significant increase in built-up areas in terms of size and extent, both, during the time span 1973–2001. The cropland and open spaces have decreased at the same time. The urban growth over the city of Mumbai has occurred mostly in the northern and western regions, with increase in both urban density and spread. This analysis supports anticipation of the emergence of satellite towns predicted by Taubenböck et al. (2012). Using module 1, the built-up areas are first predicted for the year 2010, with the MC-CA model, based on LULC conditions during the periods 1990–2001. The LULC transition indicate that during 1990–2001, the built-up areas have not converted to other types, whereas other land use classes have turned into the built-up areas. The obtained urban growth simulation for year 2010 is then cross-compared with the urban map of the same year. The kappa value is obtained as 83%, which is an indication of well-performed agreement (Landis and Koch 1977). The predicted area of built-up land cover is 331 km², which is closed to the observed estimate of 355 km². These validation results indicate that the chosen model parameters are suitable for obtaining future urbanization. Accordingly, the model is used with similar parameter settings, but using the LULC data from 2001 to 2010, to simulate the future urban growth for the years 2050.

The future pattern of urban expansion as simulated for the years 2050 is presented in Fig. 8c. Here, we consider the regulatory protection as per the environmental norms for a large protected forest area in the northern part of Mumbai city (Sanjay Gandhi National Park) as well as the wetlands along the western and southern coastal boundary of the city. The temporal assessment of built-up areas with LULC of 1973 (Fig. 4a), 2001 (Fig. 4b) and 2050 (simulated, Fig. 4c) indicate that the projected urbanization occurs mainly at the open land and croplands adjacent to the existing built up areas.
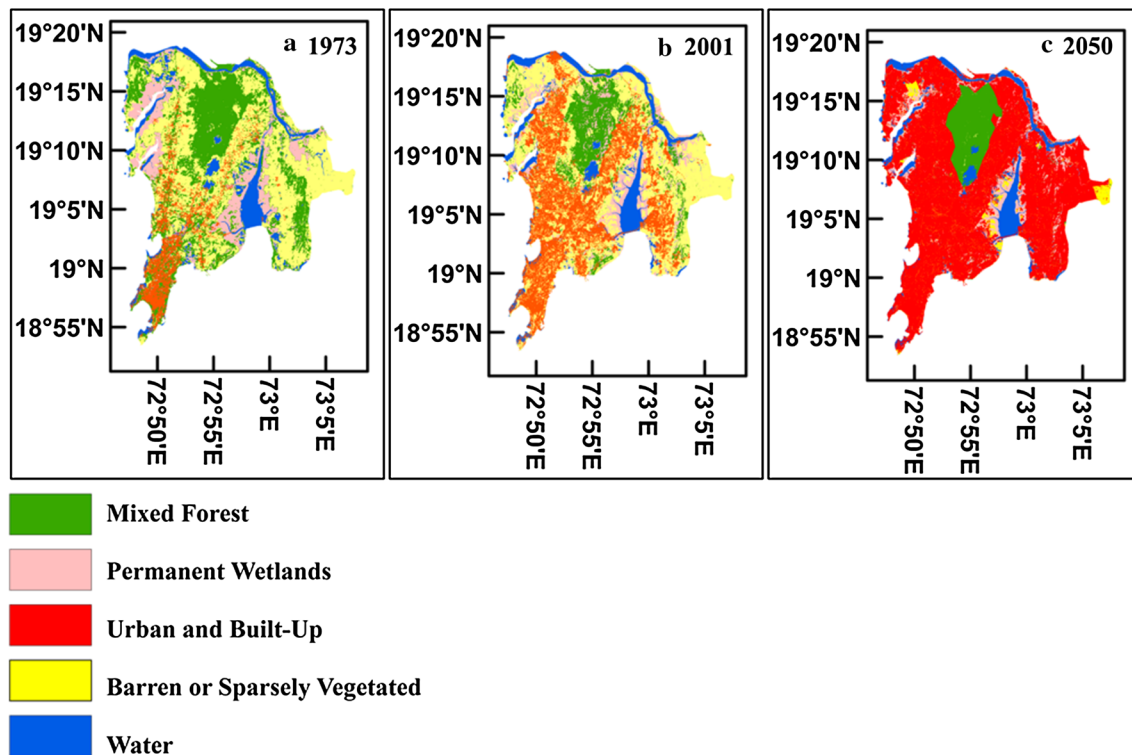
Fig. 4 Urban growth over the city of Mumbai and its Projections. Classified land use map of Mumbai for the year 1973 (**a**) and 2001 (**b**) projected growth in urbanization for 2050 (**c**)

4.2 Module 2: statistical downscaling (SD) model for climate change projections

This Module downscales the large scale projections by GCMs to fine resolution precipitation at a local scale. The first step of SD model is bias correction, which is performed for all the GCM predictor variables. The bias correction of GCM predictor variables is performed against the ERA Interim reanalysis data. We have shown the removal of bias only for surface air temperature. Figure 5c, d show the originally simulated mean and standard deviation of temperature by CCCMA, which has significant bias with respect to the ERA Interim reanalysis data (Fig. 5a, b respectively). After performing the bias correction, GCM data captures spatial variation in both mean and standard deviation (Fig. 5e, f) to resemble well with those of reanalysis data.

The SD model is first developed based on observed rainfall and climate reanalysis data, which is trained for the period 1979–1993 and tested for the period 1994–2007. The testing results are presented in Fig. 6a along with observed rainfall data (Santacruz, Mumbai) statistics. The results show that the model is capable of capturing the mean of the observed rainfall data. However, the model underestimates standard deviation, which attributes to the poor performance of models for extremes. Here, we define extreme as 95th percentile rainfall value. This also shows that extreme needs a special

treatment in SD model, which we perform using kernel regression (extreme model). The projections obtained with the kernel regression model are presented in Fig. 6b. The modified algorithm is capable of simulating extremes and hence the standard deviation also gets improved. Here we note that application of kernel regression model provides a small over estimation of extreme rainfall when applied to the GCM predictors (Fig. 6b), which is not present in the ERA Interim predictors. This difference of model performance with the reanalysis and GCM predictor data may be the result of a residual bias in the GCM data. The trained and tested kernel regression extreme projection SD model is applied to GCMs, namely CCCMA and CNRM. We obtain the rainfall projections for the historical as well as future time period for emission scenario RCP4.5 and RCP8.5. The statistical properties of future changes (difference between projected historical and future rainfall) for the city of Mumbai under the emission scenario RCP4.5 and RCP8.5 is presented with Fig. 6c, d respectively. Here, we may notice a significant uncertainty across the downscaled projections by different GCMs.

4.3 Module 3: dynamic downscaling (DD) model for assessing impacts of urbanization

This module performs the regional DD with WRF–UCM. First we validate the WRF–UCM simulations for the

Fig. 5 Bias correction methodology (standardization) applied to GCM-simulated predictors. Application of the method is demonstrated with surface level temperature. Uncorrected GCM simulations of temperature for 1969–2005: mean (**b**) and standard deviation (**e**) has significant bias with respect to the ERA interim reanalysis mean (**a**) and standard deviation (**d**). The bias corrected simulations capture spatial variation both in terms of mean (**c**) and standard deviation (**f**)
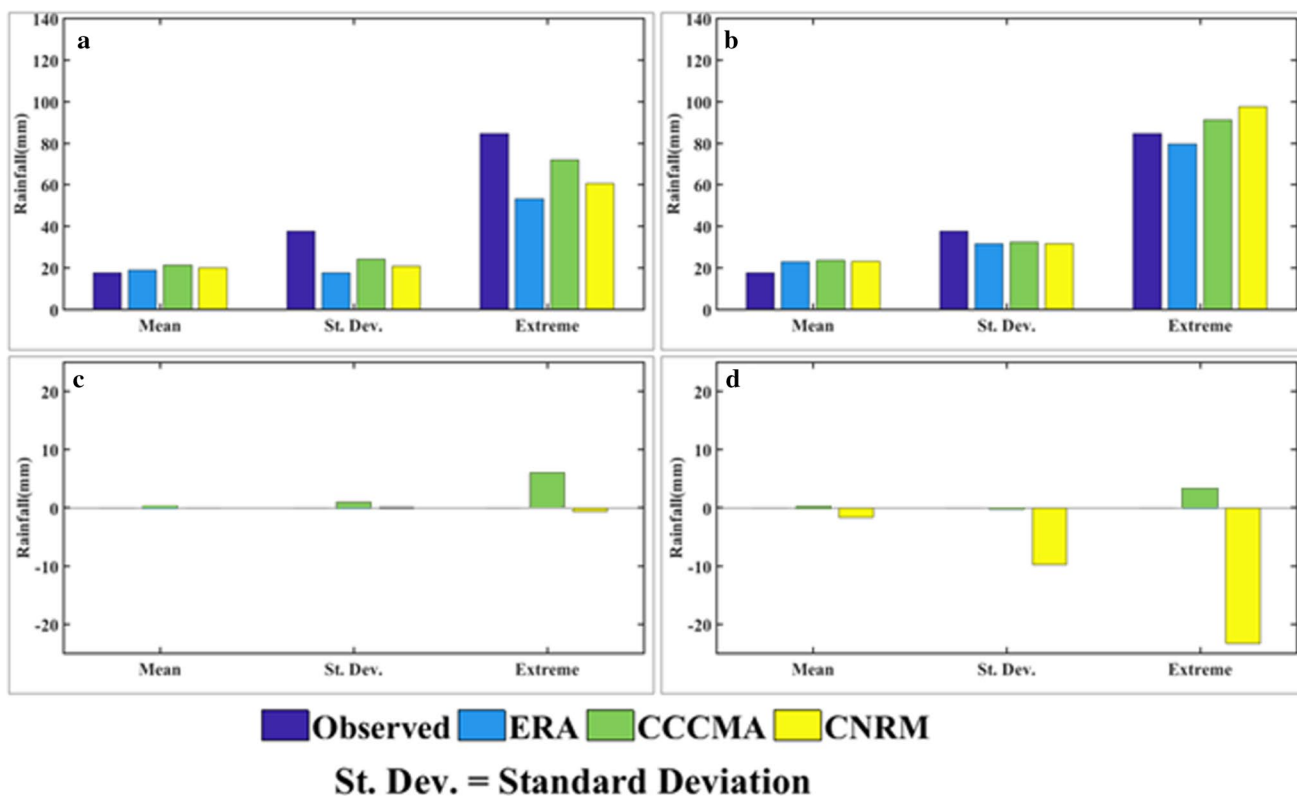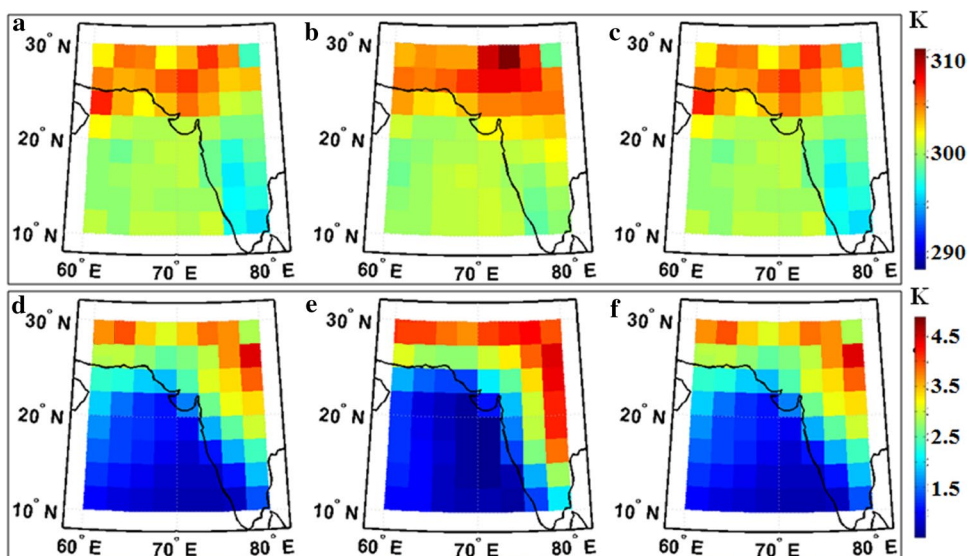

Fig. 6 Statistical properties of observed rainfall and statistically downscaled projected rainfall. Comparison of statistical properties of observed and projected rainfall (using ERA Interim reanalysis data as predictors in downscaling) for the city of Mumbai (1969–2005). **a** The projections obtained with statistical model shows that observed rainfall data and projected rainfall data are in good match in magnitude resulting low error in mean and standard deviation. However, the extremes remain largely under projected with all four GCMs. The extreme projections are effectively improved by further applying an extra regression model (**b**). The future changes in mean, standard deviation and extremes with respect to the historic time period are presented for RCP 4.5 (**c**) and RCP 8.5 (**d**)

selected 10 years. We find that the WRF–UCM overestimates the mean simulations of precipitation with respect to the observed data, when the LULC for 1973 is used (Fig. 7a). It should be noted that 1973 belongs to the training period of SD model. Any changes with respect to the simulations using 1973 LULC would show the impact of urbanization that needs to be applied to the SD output. We also find that with the present (2001) and future (2050) LULC, the mean precipitation does not change (Fig. 7a) and hence we can conclude that urbanization signature in not prominent on mean precipitation over Mumbai. Here we present the precipitation spatially averaged over all the grid points of Mumbai. The standard deviation is underestimated by the simulations with 1973 LULC and signature of urbanization on standard deviation is not so prominent for present and future LULC (Fig. 7b). WRF–UCM simulates extremes with a good accuracy when 1973 LULC is used. We also find that with present and future LULC, the extremes show significant increasing changes (Fig. 7c). Here, we note that ideally the simulations for 1997–2006 should show the best performance with the LULC for 2001, which we do not find in the present case. This clearly points the existence of bias in the regional model simulations. This is mentioned as one of the limitation. However, here we are interested in the changes in rainfall due to change in LULC. This involves subtraction of one simulation from another and this process automatically cancels the bias. Standard two sample t-test is applied to ensure the statistical significant changes in the WRF model simulated rainfall using three different urban development scenarios (pre-post-projected urbanization). The t-test confirms statistically significant changes in rainfall simulated with these three experiments at 95% significance level.

This shows the prominent urban signature in the intensification of extremes. To further examine this, we present the changes in precipitation at 5th, 25th, 50th, 75th and 95th percentiles for simulations with LULC 2001 (Fig. 8a–e, respectively) and 2050 (Fig. 8f–j, respectively) with respect to the LULC during 1973. They clearly show that at a lower quantile the impacts of urbanization on precipitation is negligible, but they become prominent at a higher quantile. The results of spatial variability of precipitation over a larger region surrounding the city of Mumbai is presented with Supplementary Figure S6. We further observe that the changes are not spatially uniform over the entire urban region. The extreme precipitation gets intensified only at a few urban pockets, which may be termed as hotspots and this needs special attention. Figure 9 identifies two hotspot regions, where the extreme precipitation is consistently intensifying with the growth of urbanization. One hotspot region is identified at Central Mumbai where the rainfall observation station Santaruz is situated (highlighted with yellow box, Fig. 9) and another in the Navi-Mumbai region (highlighted with black box, Fig. 9). The Navi-Mumbai region is the downwind urban-impacted region situated near the boundary of the protected vegetative cover of Sanjay Gandhi National Park and heavy urban development of sub-urban Mumbai. Here, it is important to note that there are increasing evidences of convective signature in the downwind urban-impacted region through complex urban land use-weather-climate feedbacks in large coastal cities, like Houston, Texas, New York, Guangzhou etc. (Changnon 1968; Landsberg 1970; Huff and Changnon 1973; Bouvette et al. 1982; Bornstein and LeRoy 1990; Orville et al. 2001; Shepherd 2005; Bornstein and Lin 2000; Schmid and Niyogi 2013; Niyogi et al. 2011;

Fig. 7 Statistical properties of observed (station: Sanacruz-Mumbai) and WRF–UCM simulated rainfall. Comparison of statistical properties between observed and simulated (WRF–UCM) rainfall over the selected 5 years with the three different land use conditions of 1973, 2001 and 2050
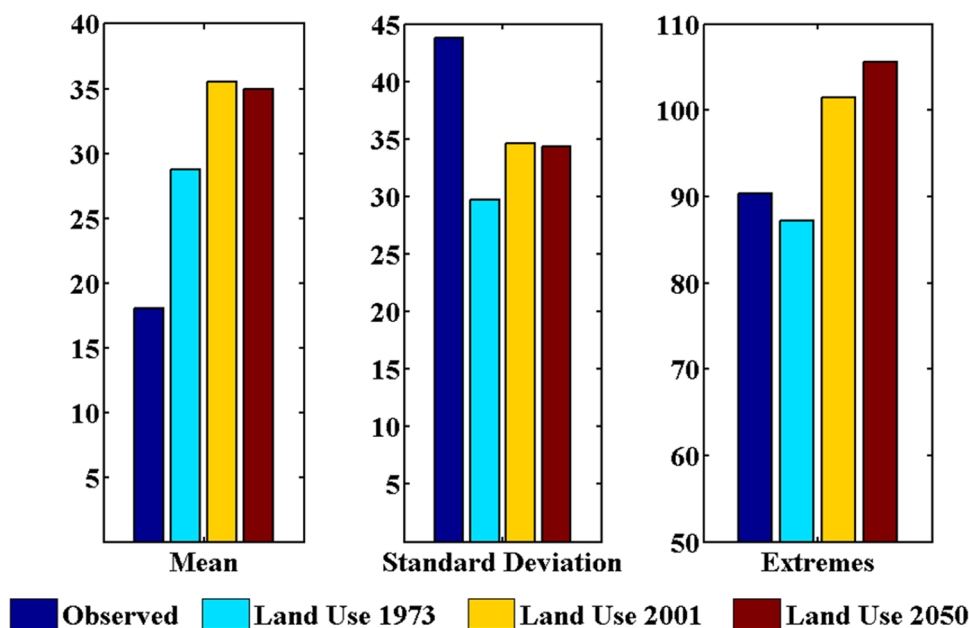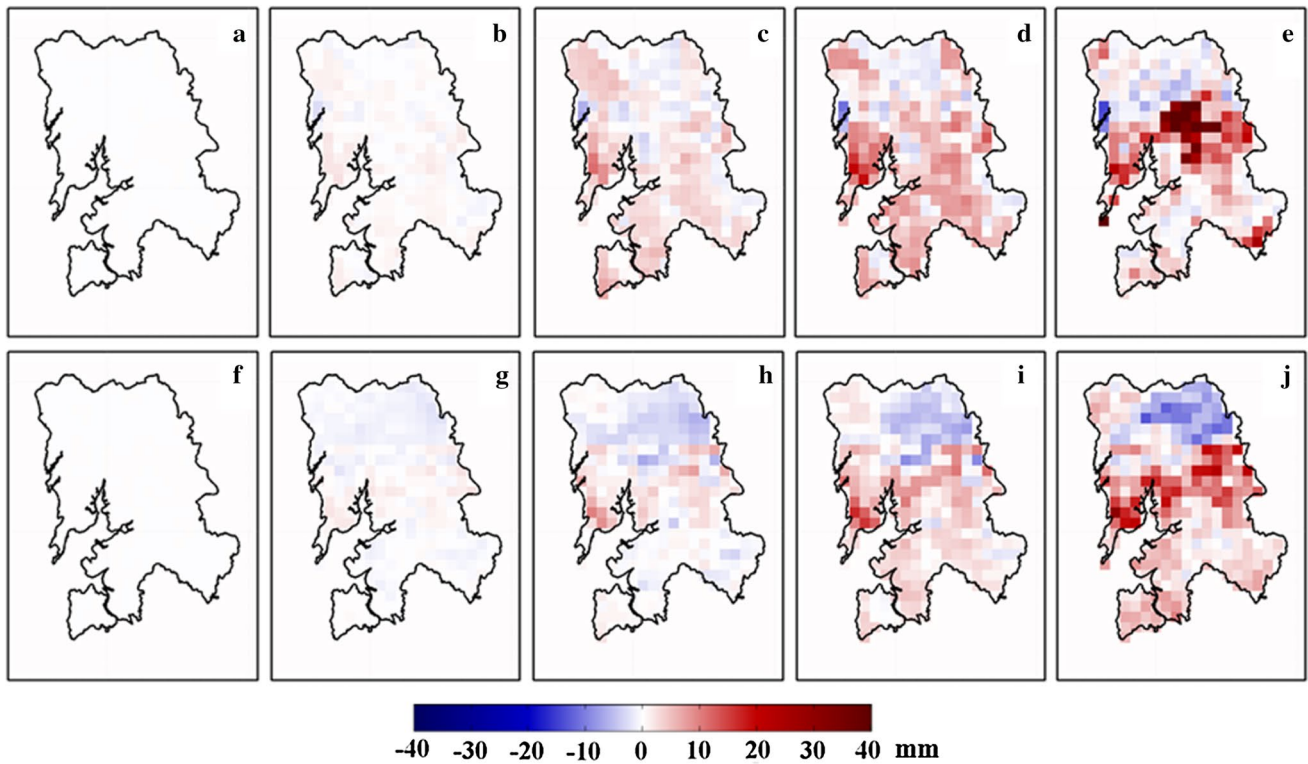
Fig. 8 The changes in rainfall characteristics and its spatial variability over the city of Mumbai with urbanization as simulated by WRF–UCM. The simulated changes in extreme precipitation due to projected future urbanization (2050–1973: Panel1-top) and present urbanization (2001–1973: Panel2-bottom) with respect to pre-urbanization (1972) period. The differences in amount of rainfall at different quantile levels reveal that the changes are non-evident over the non-extreme rainfall events (**a, f**) 5th quantile level (**b, g**) 25th quantile level (**c, h**) 50th quantile level (**d, i**) 75th quantile level, but quite prominent for extreme rainfall (**e, j**) at 95th quantile

Fig. 9 Identification of the hotspot region. The mean rainfall over a box of 16 km². where increased magnitude of extreme rainfall amount are simulated by WRF–UCM as impacts of urban growth. This is prominent for both future projected (2050) (**a**) and present urbanization (2001) (**b**) with respect to pre-urbanization (1973)
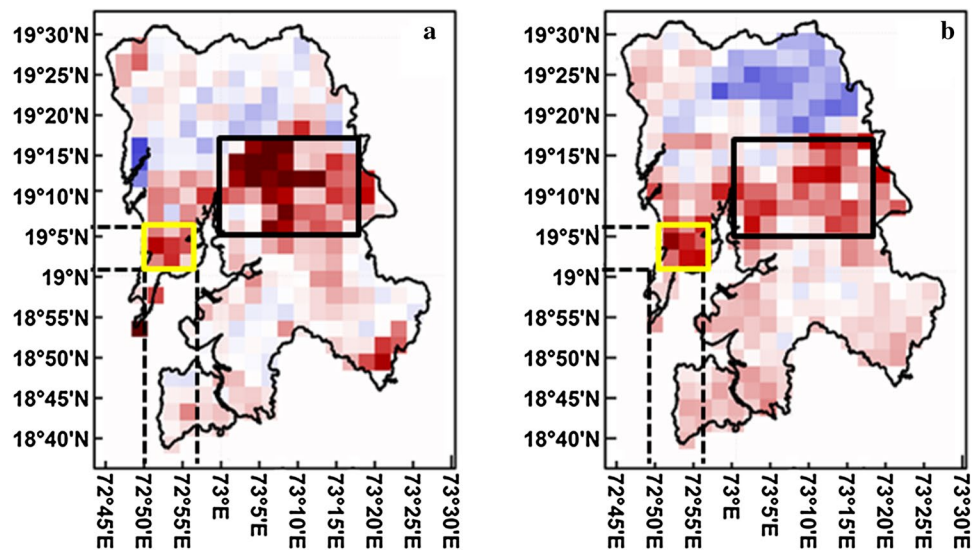
Smith and Rodriguez 2017). Our results are consistent with the literature. The results from Fig. 8 show that the rainfall in the urban region gets re-distributed with a change in spatial patterns. To further investigate the reason behind the redistribution, we observe the difference in the air temperature (Fig. 10a, f), vertical winds (Fig. 10b, g), surface heat flux (Fig. 10c, h), humidity at 850 hPa (Fig. 10d, i), and wind vectors at 850 hPa (Fig. 10e, j) between simulations with 2001 LULC and 1973 LULC (top panel) and simulations with 2050 LULC and 1973 LULC (bottom panel). We find
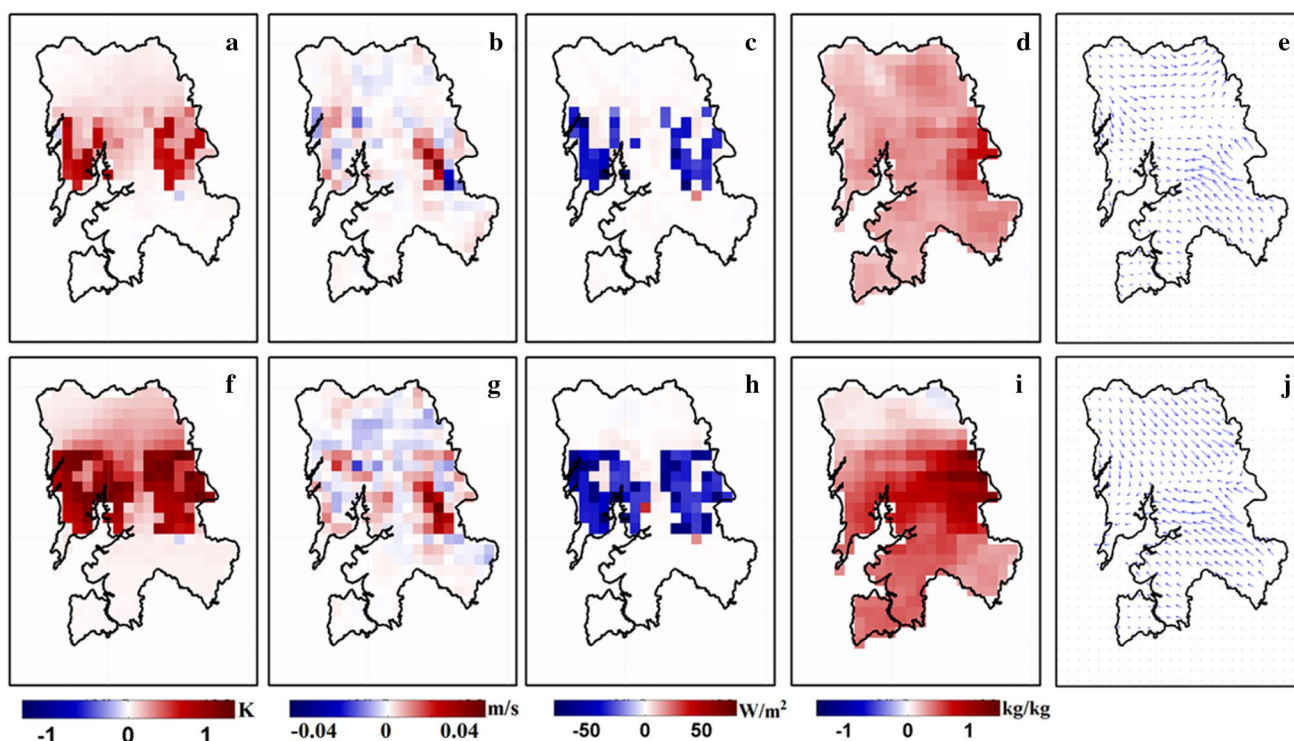
Fig. 10 The urban signature on atmospheric instability. The changes simulated by WRF–UCM in the meteorological variables over Mumbai with changed urban condition (2050–1973: Panel1-top) and pre-

sent urbanization (2001–1973: Panel2-bottom). The variables are: **a–f** 2-m air temperature, **b–g** vertical winds, **c–h** surface heat flux, **d–i** humidity at 850 hPa, **e–j** wind vectors at 850 hPa

increase in temperature over both the hotspot regions, along with a clearly visible increase in vertical velocity, heat flux and humidity under enhanced urbanization. The increase of vertical velocity signifies increase in instability that results into precipitation extremes, which is further aggravated with the higher humidity possibly due to increased temperature. We further find that the convergence of wind over both the hotspot regions of Central Mumbai and the region of Navi-Mumbai in the downwind of the city with growth of urbanization and this also favours intensified precipitation. Growth of urbanization results into perturbation in the local factors that favour intensification of extremes and all of them occur at the hotspot region.

4.4 Module 4: integration of dynamic and statistical models

This module presents results of integration of SD-DD model outputs and computation of extreme rainfall return levels. We compute the 50 years return level for extreme precipitation for 1–5 days during historic (1985–2005) and future periods (2030–2050) with integrated and SD model projected rainfall (Fig. 11). From SD simulations, we do not get any consistent changes. As for example, CCCMA (Fig. 11a) and CNRM (Fig. 11b) do not show very prominent change

in future for both RCP4.5 and RCP8.5 scenarios. When we integrate the impacts of urban growth the results change and they consistently show increase in return levels across all durations and all models. This primarily attributes to the dominant urban feedback that is shadowing the impacts of global climate change on local urban precipitation. This further shows the importance of integrating the urban feedback to the global climate change projections. Our finding calls for the re-evaluation of series of analysis (Willems et al. 2012; Markus et al. 2016; Nguyen et al. 2007; Chartlon et al. 2006; Onof and Nielsen 2009) on urban precipitation projections that consider only large scale climate change impacts and not the changes in feedbacks from land surface due to urban growth. In module 3, we are computing the possible changes in precipitation due to urbanization and this is validated in Fig. 7. The statistically downscaled products are validated in Module 2 and future changes in rainfall due to changes in synoptic scale circulation are projected. The two validated modules are combined through quantile mapping in Module 4. Module 4 does not essentially involves any statistical or dynamic model, it just adds the changes due to future urbanization to the future projected rainfall corresponding to a specific CDF vale. Hence, there is as such no specific validation for this module.

Fig. 11 Return levels of extreme precipitation with duration of 1–5 days, as projected for 2050 with (integrated) and without (statistical only) the impacts of urbanization. The GCMs considered are: **a** CCCMA, **b** CNRM
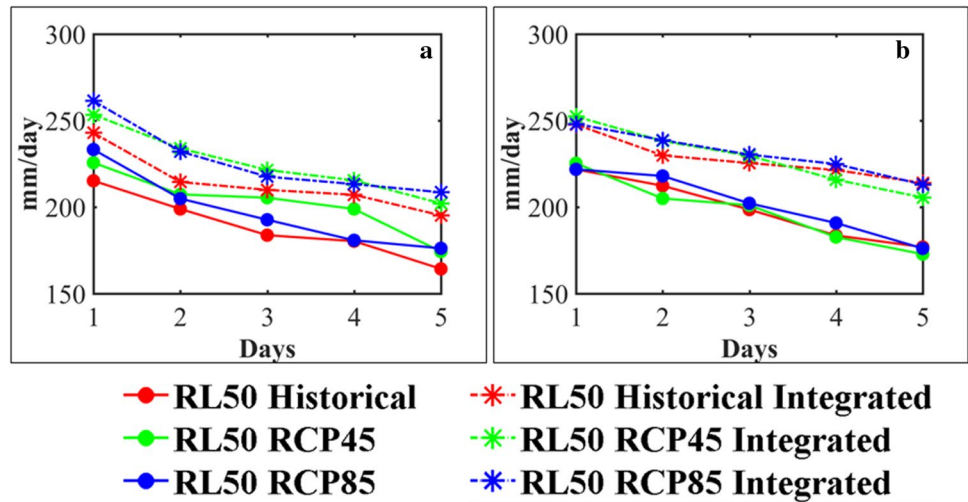
5 Summary and conclusions

Urban rainfall is changing all around the globe due to climate change and urbanization. The mechanisms behind the changes due to synoptic patterns and those due to urbanizations are different and there is likely a non-liner interaction between them. In the present analysis, we have considered this and hence, first statistically downscaled rainfall from synoptic scale circulation (Module 2). In Module 3, we obtain the likely changes in precipitation due to urbanization. We have applied those changes in Module 4 to the downscaled precipitation, rather than mixing it with the circulation pattern. One of the limitation lies in an implicit assumption that considers the changes in large scale circulation patterns due to global warming and changes due to urbanization are independent. We agree that in reality they interact with each other and this is a limitation of the model. This analysis is undertaken to estimate the effect of urban expansion of the city of Mumbai over last 30 years and further up to 2050 on the rainfall extremes. This is integrated with the downscaled climate change projections at urban scale. We extract the urban expansion and dynamics of the city of Mumbai over the last 30 years. The future urban expansion of the city further up to 2050 is obtained by an integrated MC-CA model.

The dynamical downscaling with the WRF–UCM simulation is performed with three different urbanization conditions over Mumbai. The major limitation of DD is the requirement of very high computational efficiency. In this study ten representative monsoon years are selected for dynamic model simulations. The projections obtained with limited runs of dynamic downscaled output are integrated with the SD outputs for longer term. We obtain the integrated projections for the future time period considering two different emission scenarios. We find an increase in the projected extreme rainfall with the increase urbanized

areas. The integrated methodology has ability to capture the important fine scale variations in the precipitation pattern due to the changed urbanization over the city of Mumbai. The conclusions obtained from the analysis is listed below:

1. The statistically downscaled projections of rainfall over Mumbai, as obtained from 2 different GCMs show no change; while the same is not true for extremes. CNRM show decrease, while CCCMA shows an increasing change. These projections do not consider the growing urbanization and its feedback.
2. Signature of urbanization is prominent over the city of Mumbai for extreme precipitation. The extreme events are getting intensified over few pockets of the city which are at the boundary region between the build up and forest area. The primary reason behind such intensification is the convergence of wind and increase of instability, as observed from the simulations by WRF–UCM.

The impacts of growing urbanization is dominant on the extreme events over Mumbai, as compared to the impact of large scale climate change. This results into overall increase in the future design rainfall estimates of the city, despite of a decreased climate change projection of precipitation using multiple GCMs. Here, the mechanism behind the impacts of local factors such as urbanization on precipitation works at a time scale shorter than a day. We limit our final results in representing the changes for the duration 1–5 days, and the changes are probably the summation of shorter duration changes. We agree that results will be even more significant and meaningful at a shorter time scale as shown by Paul et al. (2018). The modelling framework proposed in this study can be applied and validated for the sub-daily events, subjected to the availability of data. This may be considered as the potential area of future research.

One of the major limitation of the work is that we have not considered the sub-daily scale patterns of extremes, which is a very important factor for urban meteorology. Use of the present approach with a combination of the study performed by Chandra et al. (2015), where sub-daily scale return levels are computed, can be a potential area of future research. Findings of the study highlight the significance of computationally inexpensive integrated downscaling methodology that includes global as well as regional drivers of extremes. This approach may help to inform flood hazard preparedness and water resources management that can be easily extended for large number of urban regions to outpace the computational requirement.

References

Ahmadalipour A, Moradkhani H, Svoboda M (2016) Centennial drought outlook over the CONUS using NASA-NEX downscaled climate ensemble. Int J Climatol 37:2477

Araya YH, Cabral P (2010) Analysis and modelling of urban land cover change in Setúbal and Sesimbra, Portugal. Remote Sens 2:1549–1563

Arsanjani J, Helbich M, Kainz W, Darvishi A (2013) Integration of logistic regression, Markov chain and cellular automata models to simulate urban expansion—the case of Tehran. Int J Appl Earth Obs Geoinf 21:265–275

Azari M, Tayyebi A, Helbich M, Ahadnejad Reveshty M (2016) Integratingcellular automata, artificial neural network and fuzzy set theory tosimulate threatened orchards: application to Maragheh, Iran. GISci Remote Sens 53:183–205

Bellucci A, Haarsma R, Gualdi S, Athanasiadis PJ, Caian M, Cassou C et al (2015) An assessment of a multi-model ensemble of decadal climate predictions. Clim Dyn 44(9–10):2787–2806

Benestad RE, Mezghani A (2015) On downscaling probabilities for heavy 24-hour precipitation events at seasonal-to-decadal scales. Tellus A 67

Bornstein R, Lin Q (2000) Urban heat islands and summertime convective thunderstorms in Atlanta: three case studies. Atmos Environ 34:507–516

Bornstein R, LeRoy M (1990) Urban barrier effects on convective and frontal thunderstorms. In: Extended abstracts, Fourth Conference on mesoscale processes, pp 120–121

Bouvette TC, Lambert JL, Bedient PB (1982) Revised rainfall frequency analysis for Houston. J Hydraul Div 108(4):515–528

Burian SJ, Shepherd JM (2005) Effect of urbanization on the diurnal rainfall pattern in Houston. Hydrol Process 19(5):1089–1103

Census of India (2001, 2011) http://censusindia.gov.in/. Accessed May 2015

Chandra R, Saha U, Mujumdar PP (2015) Model and parameter uncertainty in IDF relationships under climate change. Adv Water Resour 79:127–139

Changnon SA Jr (1978) Urban effects on severe local storms at St Louis. J Appl Meteorol 17(5):578–586

Changnon SA (1968) Precipitation climatology of Lake Michigan basin. Bulletin. Illinois State Water Survey 52

Charlton R, Fealy R, Moore S, Sweeney J, Murphy C (2006) Assessing the impact of climate change on water supply and flood hazard in Ireland using statistical downscaling and hydrological modelling techniques. Clim Change 74(4):475–491

Chen F, Kusaka H, Bornstein R, Ching J, Grimmond CSB, Grossman Clarke S et al (2011) The integrated WRF/urban modelling system: development, evaluation, and applications to urban environmental problems. Int J Climatol 31(2):273–288

Cohen J (1968) Weighted kappa: nominal scale agreement provision for scaled disagreement or partial credit. Psychol Bull 70(4):213

Coles S, Bawa J, Trenner L, Dorazio P (2001) An introduction to statistical modeling of extreme values, vol 208. Springer, London

Davison AC, Smith RL (1990) Models for exceedances over high thresholds. J R Stat Soc Ser B Methodol 1:393–442

Dee DP et al (2011) The era-interim reanalysis: configuration and performance of the data assimilation system. Quart J R Meteorol Soc 125:553–597

Devanand A, Ghosh S, Paul S, Karmakar S, Niyogi D (2017) Multi-ensemble regional simulation of Indian monsoon during contrasting rainfall years: role of convective schemes and nested domain. Clim Dyn 1:1–21

Devaraju N, Bala G, Modak A (2015) Effects of large-scale deforestation on precipitation in the monsoon regions: remote versus local effects. Proc Natl Acad Sci 112(11):3257–3262

Dudhia J (1989) Numerical study of convection observed during the Winter Monsoon Experiment using a mesoscale two-dimensional model. J Atmos Sci 46:3077–3107

Eastman JR (2009) IDRISI 16: the Andes edition. Clark University, Worcester

Ganeshan M, Murtugudde R, Imhoff ML (2013) A multi-city analysis of the UHI-influence on warm season rainfall. Urban Clim 6:1–23

Ghosh S, Mujumdar PP (2007) Nonparametric methods for modelling GCM and scenario uncertainty in drought assessment. Water Resour Res 43:W07405

Ghosh S, Das D, Kao SC, Ganguly AR (2012) Lack of uniform trends but increasing spatial variability in observed Indian rainfall extremes. Nat Clim Change 2:86–91

Giorgi F (2006) Regional climate modeling: status and perspectives. J Phys IV EDP Sci (Proceedings) 139:101–118

Giorgi F, Mearns LO (1991) Approaches to the simulation of regional climate change: a review. Rev Geophys 29(2):191–216

Giorgi F, Mearns LO (1999) Introduction to special section: Regional climate modeling revisited. J Geophys Res Atmos 104(D6):6335–6352

Guan D, Li H, Inohae T, Su W, Nagaie T, Hokao K (2011) Modelling urban land use change by the integration of cellular automaton and Markov model. Ecol Model 222:3761–3772

Gupta K (2007) Urban flood resilience planning and management and lessons for the future: a case study of Mumbai, India. Urban Water J 4:3

Gutiérrez JM, San-Martín D, Brands S, Manzanas R, Herrera S (2013) Reassessing statistical downscaling techniques for their robust application under climate change conditions. J Clim 26(1):171–188

He J, Liu Y, Yu Y, Tang W, Xiang W, Liu D (2013) A counterfactual scenario simulation approach for assessing the impact of farmland preservation policies on urban sprawl and food security in a major grain-producing area of China. Appl Geogr 37:127–138

Helbich M (2012) Beyond postsuburbia? Multifunctional service agglomeration in Vienna's urban fringe. Tijdschrift voor Econ Soc Geogr 103:39–52

Hewitson BC, Crane RG (1996) Climate downscaling: techniques and application. Clim Res 7(2):85–95

Holt T, Pullen J (2007) Urban canopy modeling of the New York City metropolitan area: a comparison and validation of single- and multilayer parameterizations. Mon Weather Rev 135(5):1906–1930

Huff FA, Changnon SA Jr (1973) Precipitation modification by major urban areas. Bull Am Meteorol Soc 54(12):1220–1232

Huff FA, Changnon SA Jr (1986) Potential urban effects on precipitation in the winter and transition seasons at St Louis, Missouri. J Clim Appl Meteorol 25(12):1887–1907

Hughes JP, Guttorp P (1994) A class of stochastic models for relating synoptic atmospheric patterns to regional hydrologic phenomena. Water Resour Res 30(5):1535–1546

Hwang S, Graham WD (2014) Assessment of alternative methods for statistically downscaling daily GCM precipitation outputs to simulate regional streamflow. J Am Water Resour Assoc 50(4):1010–1032

Janjic ZI (1994) The step-mountain Eta coordinate model: further developments of the convection, viscous sublayer and turbulence closure schemes. Mon Weather Rev 122:927–945

Janjic ZI (2002) Nonsingular implementation of the Mellor-Yamada Level 25 Scheme in the NCEP Meso model. NCEP Office Note No 437:61

Jauregui E, Romales E (1996) Urban effects on convective precipitation in Mexico City. Atmos Environ 30(20):3383–3389

Kain JS (2004) The Kain–Fritsch convective parameterization: an update. J Appl Meteorol 43:170–181

Kamusoko C, Aniya M, Adi B, Manjoro M (2009) Rural sustainability under threat in Zimbabwe e simulation of future land use/cover changes in the Bindura district based on the Markov-cellular automata model. Appl Geogr 29:435–447

Kannan S, Ghosh S (2013) A nonparametric kernel regression model for downscaling multisite daily precipitation in the Mahanadi basin. Water Resour Res 49(3):1360–1385

Kannan S, Ghosh S, Mishra V, Salvi K (2014) Uncertainty resulting from multiple data usage in statistical downscaling. Geophys Res Lett 41(11):4013–4019

Kaufmann RK, Seto KC, Schneider A, Liu Z, Zhou L, Wang W (2007) Climate response to rapid urban growth: evidence of a human-induced precipitation deficit. J Clim 20(10):2299–2306

Kharin VV, Zwiers FW (2002) Climate predictions with multimodel ensembles. J Clim 15(7):793–799

Kishtawal CM, Niyogi D, Tewari M, Pielke RA, Shepherd JM (2010) Urbanization signature in the observed heavy rainfall climatology over India. Int J Climatol 30(13):1908–1916

Kraemer HC (1982) Kappa coefficient. In: Kotz S, Johnson NL (eds) Encyclopedia of statistical sciences. Wiley, New York, pp 352–354

Kundzewicz ZW, Lugeri N, Dankers R, Hirabayashi Y, Döll P et al (2010) Assessing river flood risk and adaptation in Europe—review of projections for the future. Mitig Adapt Strat Glob Change 15(7):641–656

Kusaka H, Kimuara F (2004) Coupling a single-layer urban canopy model with a simple atmospheric model: impact on urban heat island simulation for an idealized case. J Meteorol Soc Jpn 82:67–80

Kusaka H, Kondo H, Kikegawa Y, Kimura F (2001) A simple single-layer urban canopy model for atmospheric models: comparison with multi-layer and slab models. Bound Layer J Meteorol 101(3):329–358

Kusaka H, Hara M, Takane Y (2012) Urban climate projection by the WRF model at 3-km horizontal grid increment: dynamical downscaling and predicting heat stress in the 2070's August for Tokyo, Osaka, and Nagoya metropolises. J Meteorol Soc Jpn 90:47–63

Landis JR, Koch GG (1977) The measurement of observer agreement for categorical data. Biometrics 1:159–174

Landsberg HE (1970) Man-made climatic changes. Science 170(3964):1265–1274

Landsberg HE (1981) The urban climate, vol 28. Academic Press, London

Lasda O, Dikou A, Papapanagiotou E (2010) Flash flooding in Attika, Greece: climatic change or urbanization? AMBIO 39(8):608–611

Lei M, Niyogi D, Kishtawal C, Pielke Sr R, Beltrán-Przekurat A, Nobis T, Vaidya S (2008) Effect of explicit urban land surface representation on the simulation of the 26 July 2005 heavy rain event over Mumbai, India. Atmos Chem Phys Discuss 8:8773–8816

Leung LR, Qian Y, Bian X (2003) Hydroclimate of the western United States based on observations and regional climate simulation of 1981–2000 Part I: seasonal statistics. J Clim 16(12):1892–1911

Li H, Sheffield J, Eric FW (2010) Bias correction of monthly precipitation and temperature fields from Intergovernmental Panel on Climate Change AR4 models using equidistant quantile matching. J Geophys Res Atmos 115:D10

Lin CY, Chen WC, Chang PL, Sheng YF (2011) Impact of the urban heat island effect on precipitation over a complex geographic environment in Northern Taiwan. J Appl Meteorol Climatol 50(2):339–353

Mahmood R, Pielke Sr RA, Hubbard KG, Niyogi D, Bonan G et al (2010) Impacts of land use/land cover change on climate and future research priorities. Bull Am Meteorol Soc 91(1):37

Markus M, Angel J, Byard G, Zhang C, Zaloudek Z, McConkey S (2016) Communicating the impacts of potential future climate change on the expected frequency of Extreme Rainfall Events in Cook County, Illinois

Mathur S, Sharma A (2005) Mumbai floods: another wake-up call. Coordinates 1:3

Mearns LO, Arritt R, Biner S, Bukovsky MS, McGinnis S, Sain S et al (2012) The North American regional climate change assessment program: overview of phase I results. Bull Am Meteorol Soc 93(9):1337–1362

Meehl GA, Goddard L, Murphy J, Stouffer RJ, Boer G, Danabasoglu G et al (2009) Decadal prediction: can it be skillful? Bull Am Meteorol Soc 90(10):1467

Miao S, Chen F, Li Q, Fan S (2011) Impacts of urban processes and urbanization on summer precipitation: a case study of heavy rainfall in Beijing on 1 August 2006. J Appl Meteorol Climatol 50(4):806–825

Milly PC, Dunne KA, Vecchia AV (2005) Global pattern of trends in streamflow and water availability in a changing climate. Nature 438(7066):347–350

Mishra V, Lettenmaier DP (2011) Climatic trends in major US urban areas, 1950–2009, Geophys Res Lett 38:16

Mishra V, Ganguly AR, Nijssen B, Lettenmaier DP (2015) Changes in observed climate extremes in global urban areas. Environ Res Lett 10(2):024005

Mlawer EJ, Steven JT, Patrick DB, Iacono MJ, Clough CA (1997) Radiative transfer for inhomogeneous atmospheres: RRTM, a validated correlated—k model for the longwave. J Geophys Res 102:16663–16682

Monin AS, Obukhov AM (1954) Basic laws of turbulent mixing in the surface layer of the atmosphere. Contrib Geophys Inst Acad Sci USSR 151:163–187

Moss RH, Edmonds JA, Hibbard KA, Manning MR, Rose SK et al (2010) The next generation of scenarios for climate change research and assessment. Nature 463(7282):747–756

Mujumdar PP, Ghosh S (2008) Modeling GCM and scenario uncertainty using a possibilistic approach: application to the Mahanadi River, India. Water Resour Rese 44:6

Nations U (2014) World urbanization prospects: the 2014 revision, highlights (ST/ESA/SER A/352), New York

Nguyen VTV, Nguyen TD, Cung A (2007) A statistical approach to downscaling of sub-daily extreme rainfall processes for climate-related impact studies in urban areas. Water Sci Technol Water Supply 7(2):183–192

Niyogi D, Pyle P, Lei M, Arya S, Kishtawal C, Shepherd M, Chen F, Wolfe B (2011) Urban modification of thunderstorms: an observational storm climatology and model case study for the Indianapolis urban region. J Appl Meteor Climatol 50:1129–1144

Oke TR (1995) The heat island of the urban boundary layer: characteristics, causes and effects. In: Wind climate in cities, pp 81–107, Springer, The Netherlands

Oke TR, Cleugh HA (1987) Urban heat storage derived as energy balance residuals. Bound Layer Meteorol 39(3):233–245

Onof C, Arnbjerg-Nielsen K (2009) Quantification of anticipated future changes in high resolution design rainfall for urban areas. Atmos Res 92(3):350–363

Orville R, Huffines GN, Gammon J, Zhang R, Ely B, Steiger S, Phillips S, Allen S, Read W (2001) Enhancement of cloud to ground lightning over Houston, Texas. Geophys Res Lett 28(13):2597–2600

Paul S, Ghosh S, Oglesby R, Pathak A, Chandrasekharan A, Ramsankaran R (2016) Weakening of Indian Summer Monsoon rainfall due to changes in land use land cover. Sci Rep 6:32177

Paul S, Ghosh S, Mathew M, Devanand A, Karmakar S, Niyogi D (2018) Increased spatial variability and intensification of extreme monsoon rainfall due to urbanization. Sci Rep 8(1):3918

Pickands IIIJ (1975) Statistical inference using extreme order statistics. Ann Stat 3:119–131

Pontius RG, Huffaker D, Denman K (2004) Useful techniques of validation for spatially explicit land-change models. Ecol Model 179:445e461

Rose LS, Stallins JA, Bentley ML (2008) Concurrent cloud-to-ground lightning and precipitation enhancement in the Atlanta Georgia (United States), urban region. Earth Interact 12(11):1–30

Rosenfeld D (2000) Suppression of rain and snow by urban and industrial air pollution. Science 287(5459):1793–1796

Roxy MK, Ritika K, Terray P, Murtugudde R, Ashok K, Goswami BN (2015) Drying of Indian subcontinent by rapid Indian Ocean warming and a weakening land-sea thermal gradient. Nat Commun 6:7423

Saaty TL (1990) How to make a decision: the analytic hierarchy process. Eur J Oper Res 48:9–26

Saha A, Ghosh S, Sahana AS, Rao EP (2014) Failure of CMIP5 climate models in simulating post 1950 decreasing trend of Indian monsoon. Geophys Res Lett 41(20):7323–7330

Salathe EP, Mote PW, Wiley MW (2007) Review of scenario selection and downscaling methods for the assessment of climate change impacts on hydrology in the United States Pacific Northwest. Int J Climatol 27(12):1611–1621

Salvi K, Kannan S, Ghosh S (2013) High resolution multisite daily rainfall projections in India with statistical downscaling for climate change impacts assessment. J Geophys Res Atmos 118(9):3557–3578

Schilling KE, Chan KS, Liu H, Zhang YK (2010) Quantifying the effect of land use land cover change on increasing discharge in the Upper Mississippi River. J Hydrol 387(3):343–345

Schmid PE, Niyogi D (2013) Impact of city size on precipitation-modifying potential. Geophys Res Lett 40:5263–5267

Schowengerdt RA (2012) Techniques for image processing and classifications in remote sensing. Academic Press, London

Shafeezadeh Moghaddam H, Tayyebi A, Helbich M (2017) Transition index maps for urban growth simulation: application of artificial neural networks, weight of evidence and fuzzy multi-criteria evaluation. Environ Monit Assess 189:189–300

Shafizadeh MH, Helbich M (2015) Spatiotemporal variability of urban growth factors: a global and local perspective on the megacity of Mumbai. Int J Appl Earth Obs Geoinf 35(12):187–198

Shafizadeh Moghadam H, Helbich M (2013) Spatiotemporal urbanization processes in the megacity of Mumbai, India: a Markov chains-cellular automata urban growth model. Appl Geogr 40:140–149

Shashikanth K, Prashanthi M (2018) Indian summer monsoon rainfall extremes projections using block maxima approach under climate change. Int J Appl Eng Res 13(11):8925–8928

Shastri H, Paul S, Ghosh S, Karmakar S (2015) Impacts of urbanization on Indian summer monsoon rainfall extremes. J Geophys Res Atmos 120(2):496–516

Shepherd JM (2005) A review of current investigations of urban-induced rainfall and recommendations for the future. Earth Interact 9:1

Skamarock WC, Klemp JB (2008) A time-split nonhydrostatic atmospheric model for weather research and forecasting applications. J Comput Phys 227:3465–3485

Skamarock WC, Klemp JB, Duda MG, Fowler LD, Park SH, Ringler TD (2012) A multiscale nonhydrostatic atmospheric model using centroidal Voronoi tesselations and C-grid staggering. Mon Weather Rev 140(9):3090–3105

Smith B, Rodriguez S (2017) Spatial analysis of high-resolution radar rainfall and citizen-reported flash flood data in ultra-urban New York City. Water 9(10):736

Song X, Zhang J, AghaKouchak A, Roy SS, Xuan Y, Wang G et al (2014) Rapid urbanization and changes in spatiotemporal characteristics of precipitation in Beijing metropolitan area. J Geophys Res Atmos 119:11

Srinivas CV, Hariprasad D, Bhaskar Rao DV, Anjaneyulu Y, Baskaran R, Venkatraman B (2013) Simulation of the Indian summer monsoon regional climate using advanced research WRF model. Int J Climatol 33(5):1195–1210

Tachikawa T, Kaku M, Iwasaki A, Gesch D, Oimoen M, Zhang Z et al (2011) ASTER global digital elevation model version 2—summary of validation results, August 31, 2011

Taubenböck H, Esch T, Felbier A, Wiesner M, Roth A, Dech A (2012) Monitoring urbanization in mega cities from space. Remote Sens Environ 117:162–176

Taylor KE, Stouffer RJ, Meehl GA (2012) An overview of CMIP5 and the experiment design. Bull Am Meteor Soc 93(4):485

Tewari M, Chen F, Wang W, Dudhia J, LeMone MA et al (2004) Implementation and verification of the unified NOAH land surface model in the WRF model 20th conference on weather analysis and forecasting/16th conference on numerical weather prediction, pp 11–15

Thompson G, Paul RF, Roy MR, William DH (2008) Explicit forecasts of winter precipitation using an improved bulk microphysics scheme Part II: implementation of a new snow parameterization. Mon Weather Rev 136:5095–5115

Trenberth KE (2011) Changes in precipitation with climate change. Clim Res 47(1–2):123–138

Trusilova K, Jung M, Churkina G, Karstens U, Heimann M, Claussen M (2008) Urbanization impacts on the climate in Europe: numerical experiments by the PSU-NCAR Mesoscale Model (MM5). J Appl Meteorol Climatol 47(5):1442–1455

Vittal H, Karmakar S, Ghosh S (2013) Diametric changes in trends and patterns of extreme rainfall over India from pre-1950 to post-1950. Geophys Res Lett 40(12):3253–3258

Vuuren VDP, Edmonds J, Kainuma M, Riahi K, Thomson A, Hibbard K et al (2011) The representative concentration pathways: an overview. Clim change 109:5–31

United Nations, Department of Economic and Social Affairs, Population Division (2011) World population prospects: the 2010 revision, vol I. Comprehensive tables. ST/ESA/SER.A/313

Wai KM, Wang XM, Lin TH, Wong MS, Zeng SK, He N, Wang DH (2017) Observational evidence of a long-term increase in precipitation due to urbanization effects and its implications for sustainable urban living. Sci Total Environ 599:647–654

Wentz FJ, Ricciardulli L, Hilburn K, Mears C (2007) How much more rain will global warming bring? Science 317(5835):233–235

White R, Engelen G (1997) The use of constrained cellular automata for high resolution modelling of urban land-use dynamics. Environ Plan A 24:323–343

Wilby RL, Wigley TML (1997) Downscaling general circulation model output: a review of methods and limitations. Prog Phys Geogr 21(4):530–548

Wilby RL, Wigley TML (2000) Precipitation predictors for downscaling: observed and general circulation model relationships. Int J Climatol 20:641–661

Wilby RL, Charles SP, Zorita E, Timbal B, Whetton P, Mearns LO (2004) Guidelines for use of climate scenarios developed from statistical downscaling methods, pp 1–27

Willems P, Arnbjerg-Nielsen K, Olsson J, Nguyen VTV (2012) Climate change impact assessment on urban rainfall extremes and urban drainage: methods and shortcomings. Atmos Res 103:106–118

Zahmatkesh Z, Karamouz M, Goharian E, Burian SJ (2014) Analysis of the effects of climate change on urban storm water runoff using statistically downscaled precipitation data and a change factor approach. J Hydrol Eng 20(7):05014022

Zhang X, Zwiers FW, Hegerl GC, Lambert FH, Gillett NP et al (2007) Detection of human influence on twentieth-century precipitation trends. Nature 448(7152):461–465